

Fabrication of silicon W and G center embedded light-emitting diodes for electroluminescence

Nikki Ebadollahi^{1a)}, Pradeep N. Namboodiri², Christian Pederson¹, Vijin Kizhake Veetil³, Marcelo I. Davanco², Kartik A. Srinivasan², Aaron M. Katzenmeyer², Matthew Pelton³, Joshua M. Pomeroy²

¹University of Maryland, College Park, MD 20742, USA

²National Institute of Standards and Technology, Gaithersburg, MD 20899, USA

³University of Maryland, Baltimore County, MD 21250, USA

a) Electronic mail: nikki.ebadollahi@nist.gov

The need for reliable quantum light sources drives our research to study color centers (CCs) in silicon as telecommunications O-band emitters. Building from photoluminescence (PL) measurements, we compare new electroluminescence (EL) measurements. To this end, we synthesized CC-embedded p-i-n junctions in silicon, creating CC light-emitting diode (CC-LED) devices. The two types of CCs synthesized were G-centers and W-centers, which show zero-phonon lines (ZPLs) at approximately 1279 nm and 1218 nm, respectively. Here, we present our device design, fabrication process flow, and report on the device performance results from measurements to date.

I. INTRODUCTION

Silicon color centers are point defects that can facilitate direct recombination upon excitation. They emit at wavelengths within the telecom band, making them interesting prospects for telecom quantum light sources^{1,2,3}. In order to emit efficiently, these defect centers must be cooled down to the cryogenic regime at temperatures below 30 K⁴. Phonon scattering and non-radiative mechanisms that dominate at room temperature are significantly reduced at cryogenic temperatures, allowing for efficient emission into the zero-phonon line (ZPL)⁵.

We have synthesized W and G color centers (CCs). W-centers are composed of three silicon interstitials and a vacancy⁶. The W-centers were created by implanting Si(28)+ ions at 65 keV with a $5 \times 10^{12} \text{ cm}^{-2}$ dose into a silicon-on-insulator (SOI) wafer. A post-implantation anneal is performed to complete W-center formation. G-centers are composed of two substitutional carbon atoms and a silicon interstitial^{7,8}. The G-centers were created by implanting C(12)+ ions at 35 keV with a $4 \times 10^{13} \text{ cm}^{-2}$ dose into the SOI⁹. The anneal time and temperature required differ for the W and G centers. A longer duration, lower temperature anneal is typical for W-center formation, while a shorter duration, higher temperature anneal is more common for G-center formation.

To verify the successful synthesis of color centers, photoluminescence measurements are commonly used⁴. For our measurements, a 635 nm laser was used to excite the color center implanted regions on a wafer. The emitted light was collected by a spectrometer or was integrated as a function of position on the surface to create an intensity map. By analyzing the ZPLs collected in the spectra, the type of color centers can be identified. We are moving to electrically pumping the CCs, by taking advantage of both the electrical and optical properties of silicon to electrically pump them using p-i-n junctions, thereby forming CC light-emitting diodes (LEDs)¹⁰. Thus, these CC-LEDs could potentially provide a mechanism by which light can be coupled from CCs to quantum dots. This paper reports on the design, synthesis, and functionality of CC-embedded LEDs to ultimately allow for electroluminescence from W- and G-centers.

II. EXPERIMENTAL

A. *Device Design*

The CC-LED (color center light emitting diode) devices were fabricated on two silicon-on-insulator (SOI) wafers, one with W-centers and the other with G-centers. Each wafer contains 49 dies and each die contains 12 CC-LED devices as shown in Figure 1a. Three parameters of the device designs were varied: 1) the color center implant window width, 2) the ohmic implant width, and 3) the separation or overlap between the ends of opposing p- and n-type ohmic regions (p-i-n or p-n devices, respectively). Figure 1b shows an overview of the layout of one device, highlighting the trenches and area within which the CC ions are implanted. The implant window width is the area implanted with ions for color center synthesis, as seen in Figure 1c. The ohmic width is the same for both the n-type and p-type regions in the diode fine structure within a device. This figure also shows these three device design degrees of freedom. The width of the fin is 9 μm for all devices.

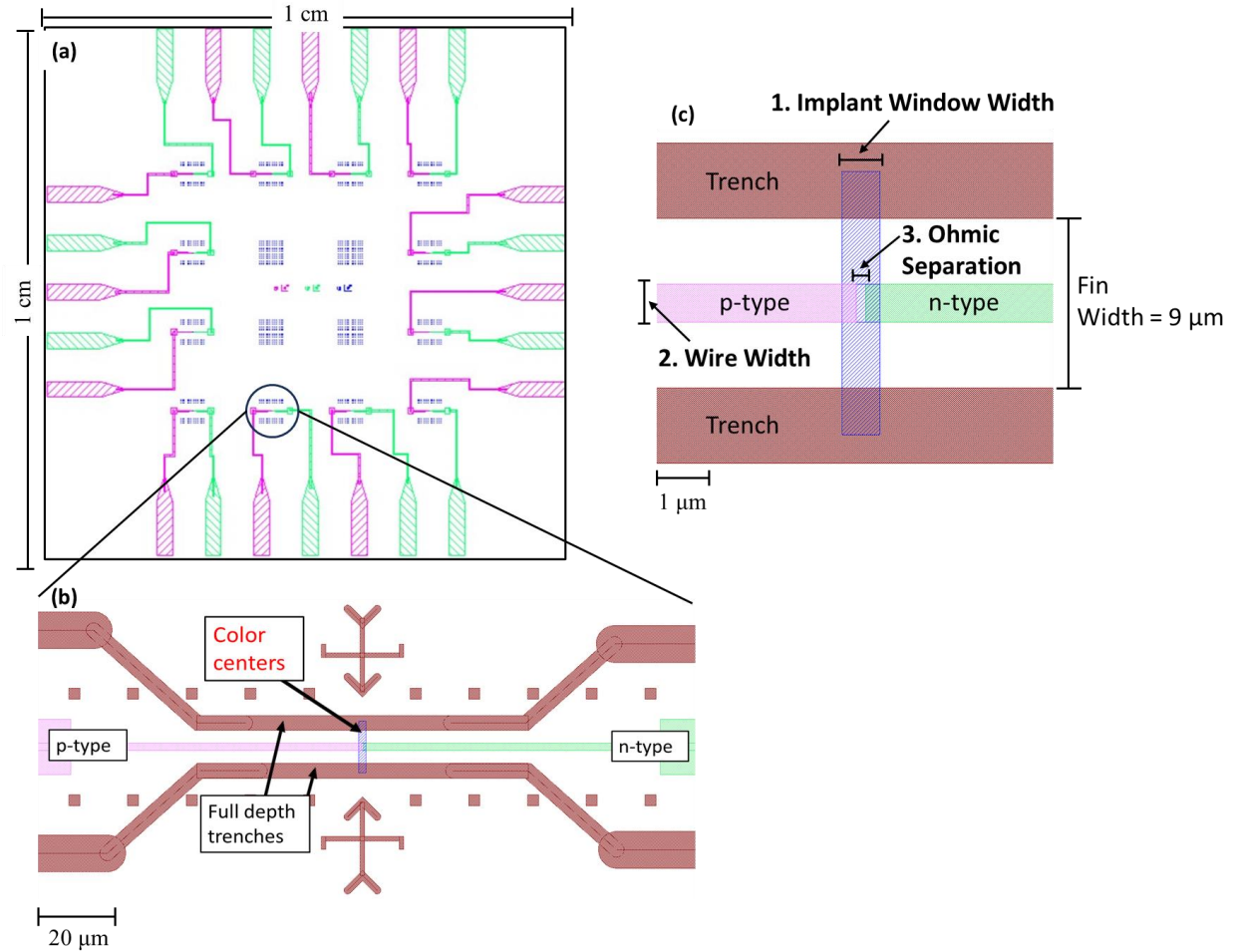


FIG. 1. a) The 1 cm x 1 cm die layout consisting of 12 individual CC-LED devices. The pink and green regions represent the p- and n-type regions, respectively. These ohmic regions meet at the device region, which is circled for one of the devices on the die. The trenches and fiducials are omitted in this figure to enhance clarity. b) A zoomed in view of an example device, illustrating the typical layout in the fine structure. c) A labeled diagram of a CC-LED device showing the three design degrees of freedom.

The implant window width and wire width are the same within any given die, but vary from die to die, while the separation of the ohmic regions varies across the 12 devices in the same pattern on all dies. Table 1 shows the values used for these parameters. An implant window width of 0 μm means no ions were implanted. When the ohmic region separation width is 0 μm, then the device was designed to have an abrupt

p-n junction. The positive ohmic region separation values indicate p-i-n devices, while the negative values signify overlap between the p and n regions. The wafer contains all the different combinations of these three degrees of freedom across the wafer. Thus, each device has a different set of implant window widths, wire widths and ohmic separation values.

TABLE I. The values used for three design degrees of freedom in the devices on the wafer. All combinations were fabricated.

Implant Window Width (μm)	0, 2, 3, 5, 10
Wire Width (μm)	2, 3, 5
Ohmic Separation (μm)	-3.0, -2.0, -1.5, -1.0, -0.5, 0, +0.5, +1.0, +1.5, +2.0, +3.0, +5.0

B. Device Fabrication

Most of the device fabrication steps apply to both the W and G center wafers; however, differences between the synthesis of the two CC types and lessons learned along the way led to some variations and rework. The devices were fabricated on SOI wafers with a 220 nm thick device layer and 3 μm buried oxide layer. In both wafers, the first step in fabricating the CC-LED devices is to etch the global alignment marks, location marks for microscopy and the electrical trench isolation using standard optical lithography and the Bosch etch process. Dry thermal oxidation at 950 $^{\circ}\text{C}$ for 1 hour was used to grow about 25 nm of oxide to passivate the surfaces. Next, the windows for the n-type implant were patterned, followed by implanting with phosphorous ions at 30 keV and $5 \times 10^{15} \text{ cm}^{-2}$. This process was then repeated for the p-type regions with a boron ion

implant at 25 keV and $5 \times 10^{15} \text{ cm}^{-2}$. Next, a 900 °C anneal was done for 1 min to activate the implants. To allow electrical contacts, openings were lithographically defined and the passivation oxide was etched using buffered oxide etch (BOE) for 5 min. Metal contacts were then made to the devices by depositing a 300 nm thick layer of aluminum using electron beam evaporation into the etched areas. To form the contacts, a 425 °C spike anneal was done to allow for aluminum spiking. This was followed by patterning windows for implanting the color center ions. This area is centered in the intrinsic region between the p-type and n-type doped areas. From this point in the process onward, the W-center and G-center wafer processes diverge.

The W-center wafer was implanted with silicon ions at 65 keV at $5 \times 10^{12} \text{ cm}^{-2}$ followed by a 250 °C anneal in a N_2 ambient environment for 30 minutes to enable W-center formation. Electron beam evaporation was then used to deposit a Ti-Au-Ti layer (5 nm-130 nm-5 nm) onto the aluminum contacts to make bond pads for electrical characterization of the devices. The wafer was then diced into individual dies. Upon attempting to package the W-center dies for testing, wire bonding to the Ti-Au-Ti contact pads was difficult due to the hardness of titanium. To overcome this challenge, the contact pads were reworked to add a Ti-Au layer (5 nm-130 nm) using the electron beam evaporator, which enabled successful wire bonding.

After the patterning of windows for the CC implant regions, the G-center wafer was implanted with carbon ions at 35 keV at $4 \times 10^{13} \text{ cm}^{-2}$. The aluminum pads were etched out for compatibility with the high temperature anneal furnace. The high temperature anneal with a quick ramp (1000 °C for 5 s, 100 deg/s) was then done to form G-centers. This high ramp anneal is intended to control the density of single G-center formation and

to increase the signal-to-background ratio¹¹. The wafer was then diced into 8 sections to vary the annealing conditions for G-center formation and test which would efficiently yield CCs. For the devices presented here, the contact pads were patterned and palladium was deposited and annealed at 250 °C in an argon gas ambient environment for 5 min to form a silicide. A Ti-Au (10 nm-250 nm) metal contact was then deposited onto the pads using electron beam evaporation before dicing the split into individual dies. Figure 2 shows micrographs of one device after undergoing the entire fabrication process.

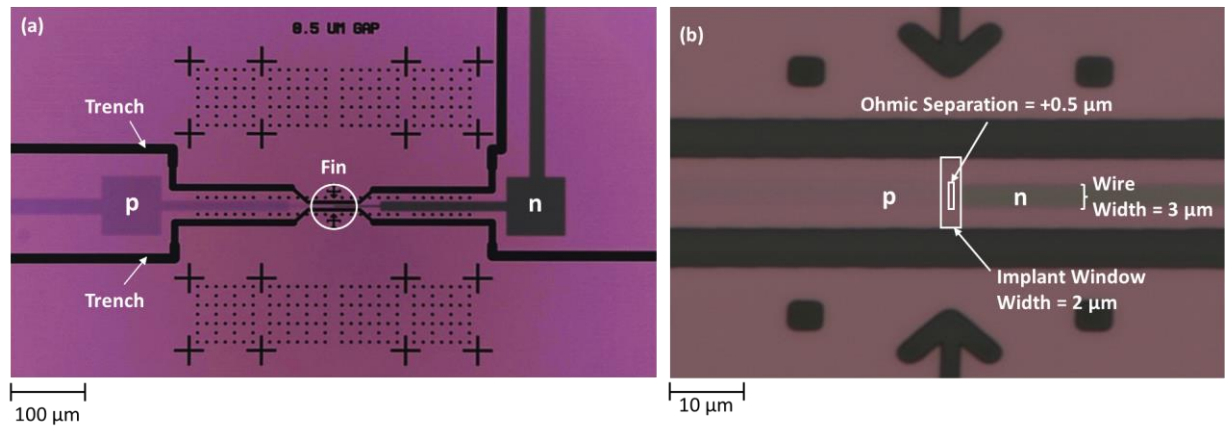


FIG. 2. a) Micrograph of one CC-LED device showing the fin area (circled) at the center of the p-type (pink) and n-type (green) ohmic regions. Trenches (dark brown) surround the ohmics to allow for current confinement. b) The fin region of the same device as in (a) showing the implant window area and ohmic separation (gap) region. This device has a 2 μm implant window width, 3 μm wire width and +0.5 μm ohmic separation.

III. RESULTS AND DISCUSSION

For measurements, individual dies were packaged onto custom printed circuit boards (PCBs). The TiAu pads on the die were wire bonded to the contacts on the PCB to provide individual p- and n-type contacts to all 12 devices on a die. The PCB was mounted onto a copper block and put into a large cryocooler system. The preliminary measurements were I-V (current-voltage) swept for each device measured at room

temperature and then cooled down and repeated at 4 K. These electrical measurements assess how the diodes perform and reveal trends in how the various splits affect the diode behavior. Additionally, a germanium photodiode overlapping all the devices was positioned directly over the die to measure luminescence. When driving a current through each device, the photodiode measured how much light is produced. The photocurrent provides the brightness of each device. These measurements were done at both room and cryogenic temperatures. All the devices on a die could be measured during one cool down cycle, allowing for an efficient way to analyze and compare the different splits. Having screened which devices emit light and the brightness of the light, the next step is to determine whether the light is due to color centers. In order to do so, some samples were mounted in an optical cryostat and the emission spectra were measured.

A. *Electrical Characterization*

The CC-LED devices were initially tested with respect to how they operate as diodes. These preliminary measurements were done to assess the effect of temperature, the role of implants intended for color center formation, and design parameters on the device's electrical performance. Since color centers are only able to emit efficiently in the cryogenic regime, a comparison was first made between a device's electrical performance at room temperature and at 4 K. Figure 3a shows the current as a function of the voltage swept across an LED device with corrections for a low temperature parasitic resistance of 3.2 k Ω across the device which is the resistance across the long source and drain leads. The corrected voltage is calculated using the equation: $V_{\text{corrected}} = V_{\text{raw}} - I \cdot R_p$. This device has no CCs implanted and was measured at both room temperature and 4 K, as depicted by the red and blue lines, respectively. The device has a 0 μm wide implant window (no

CCs), 2 μm wire width and a 0 μm separation between the p- and n-type ohmic regions. This comparison between the RT versus 4 K data for a control device without CCs serves to demonstrate that in the cryogenic regime, the threshold voltages in the LED devices shift to higher voltages.

Next, we compare devices at room temperature and 4 K that contain color centers while varying only the ohmic separations. The I-V curves of W-center CC-LED devices using the corrected voltages are shown in Figure 3b for five devices with different ohmic separation values at RT and 3 K. The low temperature parasitic resistances across these 5 devices used to correct the voltages are 3.5 k Ω , 3.7 k Ω , 2.9 k Ω , 3.2 k Ω and 3.4 k Ω for the -1.0 μm , -0.5 μm , 0 μm , +0.5 μm and +1.0 μm devices, respectively. This data generally demonstrates that as the separation between the p- and n-type ohmic regions increases, the threshold voltage (V_{th}) increases. Furthermore, as also seen in Figure 3a for the devices without CCs, these devices in Figure 3b shift to higher threshold voltages at cryogenic temperatures. Thus far, the devices with gaps between the ohmics (p-i-n devices) pass smaller currents while the devices with overlapping ohmics (p-n devices) or the no gap (0 μm) device pass larger currents.

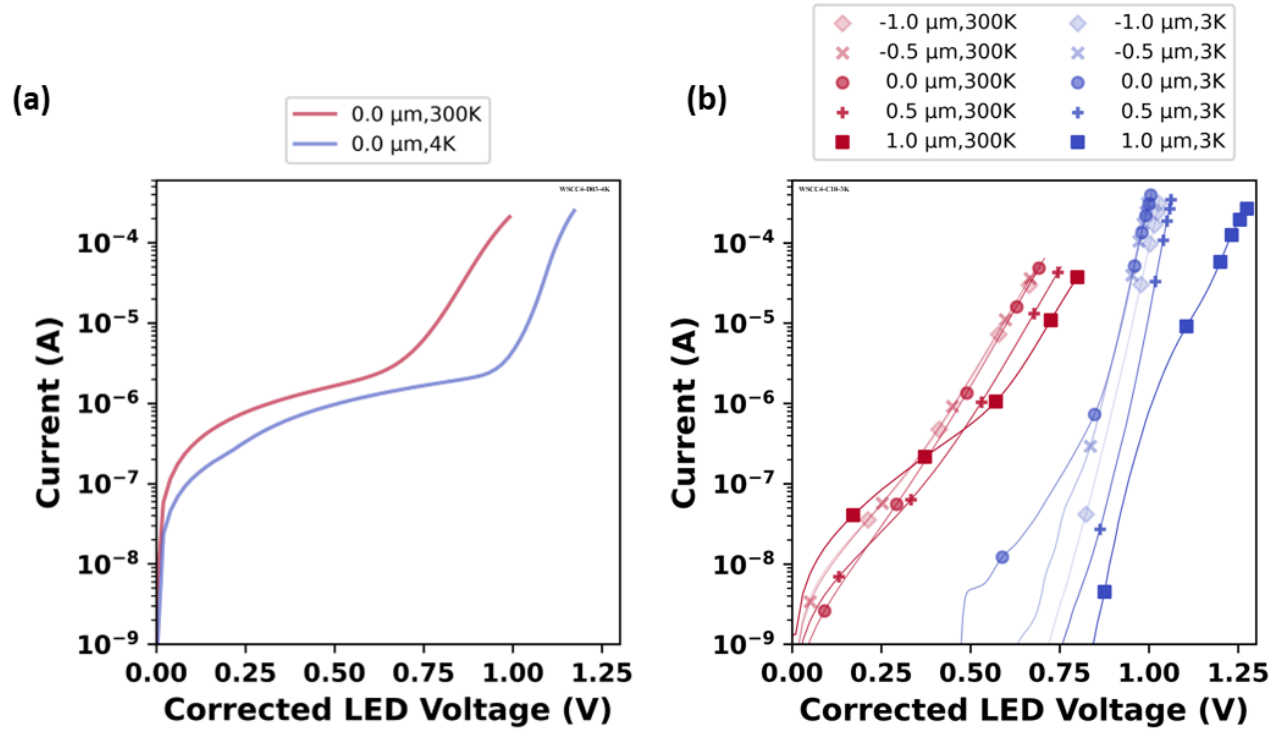


FIG. 3. a) The I-V of a device without CCs at room temperature (RT) and 4 K on a semi-log scale showing the temperature dependent threshold shift. This device has a $0 \mu\text{m}$ implant window width (no CCs implanted), a $2 \mu\text{m}$ wire width and $0 \mu\text{m}$ ohmic separation. b) A comparison between the I-Vs of W-center CC-LEDs with a $2 \mu\text{m}$ implant window width, $5 \mu\text{m}$ wire width and varying ohmic separations measured at 300 K and 3 K. As seen, larger gaps have higher thresholds. Uncertainties in the current are $<1 \text{ nA}$.

B. Electroluminescence Intensity

The I-V curves in Figure 3 provide a qualitative way to assess the electrical performance of the CC-LEDs. The next step is to measure the light being generated from these devices. To do this, a large area germanium photodiode was positioned directly over the die, placed into a cryocooler system and cooled down to 3 K. As shown in Figure 4a, as the W-center CC-LED went above threshold, a photocurrent was observed from the photodiode. This device has a $2 \mu\text{m}$ implant window width, a $5 \mu\text{m}$ wire width

and a $+1.5\ \mu\text{m}$ ohmic separation (gap) with a $3.4\ \text{k}\Omega$ parasitic resistance (accounted for in the voltage). The electro-optic efficiency of the device is calculated as the ratio between the power collected by the photodiode to the power consumed by the LED, as shown in Figure 4b. Estimated uncertainties are represented by selected error bars. This demonstrates that the CC-LED devices do emit light, motivating then to compare the brightness of the devices for the various splits. Using the germanium photodiode to measure all 12 devices on a die in one cool down cycle allowed for ease in comparing different device designs. Figure 4c shows the intensity of the light collected from several W-center CC-LED devices with a $2\ \mu\text{m}$ implant window width, a $5\ \mu\text{m}$ wire width and varying ohmic separations with $100\ \mu\text{W}$ of LED power. The W-center CC-LEDs with the overlapping p- and n-type regions (p-n devices) are the dimmest, while devices with a gap between the ohmic regions (p-i-n devices) are the brightest devices. We were able to mount a chip of W-center devices into an optical cryostat system connected to a spectrometer and measure the electroluminescent (EL) spectra. This measurement was conducted with a W-center embedded device with a $2\ \mu\text{m}$ implant window width, a $5\ \mu\text{m}$ wire width and $1.5\ \mu\text{m}$ ohmic separation. As shown in Figure 4d, the collected spectra shows a ZPL at approximately $1218\ \text{nm}$ verify W-center emission. Figure 4c showed that the devices with the ohmic gaps (p-i-n devices) produced the largest photocurrents and thus, the brightest light. The electroluminescence measurement confirms that the light from a $1.5\ \mu\text{m}$ gap device is emitted from the W-centers, as the $1218\ \text{nm}$ ZPL acts as a distinct feature for identifying this type of CCs.

This is the author's peer reviewed, accepted manuscript. However, the online version of record will be different from this version once it has been copyedited and typeset.
PLEASE CITE THIS ARTICLE AS DOI: 10.1116/6.0004055

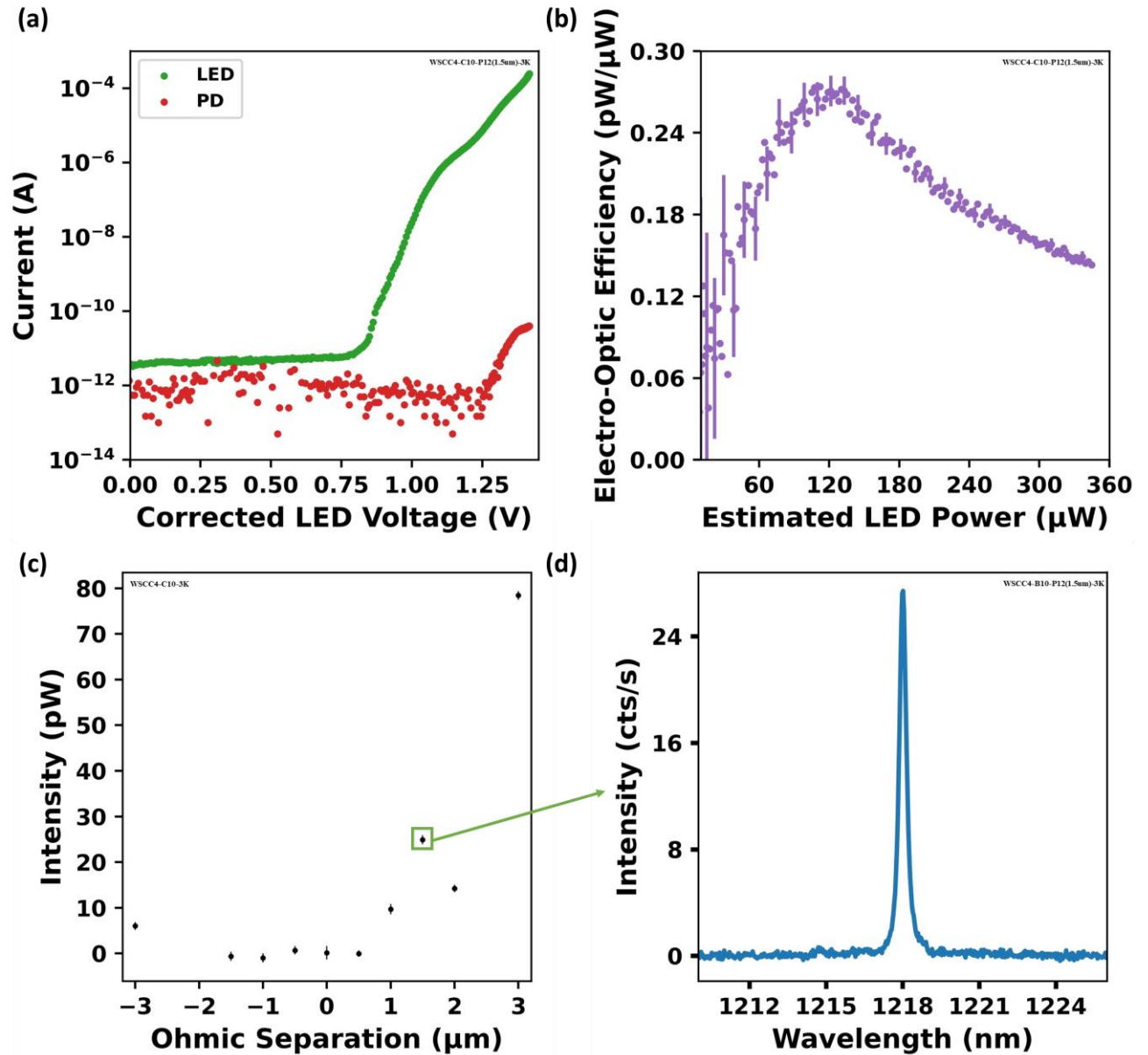


FIG. 4. a) The I-V behavior of a W-center CC-LED and photocurrent on a germanium photodiode as a function of the corrected voltage at 3 K is shown. The parasitic resistance in this device is 3.4 k Ω . This device has a 2 μ m implant window width, a 5 μ m wire width and a +1.5 μ m ohmic separation. b) The efficiency of the LED is the ratio of power collected by the photodiode to the power consumed by the LED as a function of LED power for the device in Figure 4a. The uncertainty in the currents is approximately 1 pA. The current flowing through this CC-LED device at 100 μ W of power was 74 μ A. c) The optical power from 10 devices on the same W-center die with a 2 μ m implant window

width and a 5 μm wire width shown as a function of ohmic separation at 100 μW . Estimated uncertainty in the measured power is represented by the selected error bars. d) The electroluminescent (EL) spectra as a function of wavelength for a W-center CC-LED device with a 2 μm implant window width, a 5 μm wire width and a +1.5 μm ohmic separation (same device parameters as the circled device in Figure 3c). The ZPL at 1218 nm was measured at 3 K using a 68 μA current source with a 1.7 V uncorrected bias across the LED and 180 s integration time.

From the second wafer, the G-center LED devices show I-V behavior at 3 K with a comparable trend to that of the W-center devices shown in Figure 3c. The I-V curves of G-center CC-LED devices are shown in Figure 5a for five devices all of which have a 3 μm implant window width, 3 μm wire width and varying ohmic separations. The voltage in Figure 5a is the corrected voltage with a low temperature parasitic resistance of 3.7 k Ω , 3.9 k Ω , 3.4 k Ω , 4.1 k Ω and 5.3 k Ω for the -3.0 μm , -1.0 μm , 0 μm , +1.0 μm and +3.0 μm devices, respectively. A comparison between Figure 3b for the W-center devices and Figure 5a for the G-center devices demonstrates that the CC-LEDs electrically behave similarly to an applied voltage for both types of CC. However, when measuring the optical response of the G-center CC-LEDs, as shown in Figure 5b, the light intensity produced by the devices as a function of the intrinsic region width shows a noticeably different trend than that of the W-center devices shown in Figure 4c. This photocurrent data was obtained for 11 G-center devices with comparable design degrees of freedom as the W-center device measured in Figure 4c (3 μm implant window width, 3 μm wire width and varying ohmic separations). Figure 5b shows that the G-center CC-LEDs are much brighter overall for those with overlapping ohmics (p-n devices) than those with the gap between the ohmics (p-i-n devices), which is opposite to what was seen for the W-center devices. This difference could indicate that the light from the G-center devices is

not coming from the CCs and could potentially be from band edge emission from the silicon. However, the spectroscopic measurements of the G-centers remains a work in progress.

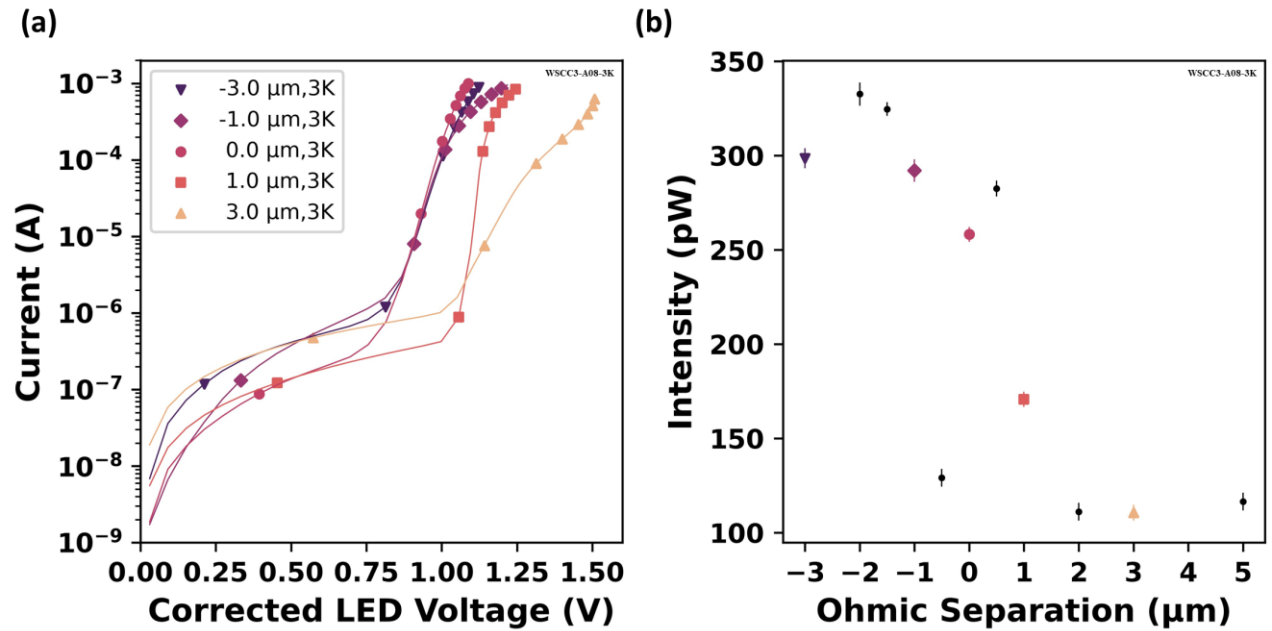


FIG. 5. a) A comparison between the I-V behavior of G-center CC-LEDs on a single die with varying ohmic separations measured at 3 K on a semi-log scale. The implant window width and wire width for all 5 of these devices are 3 μm and 3 μm , respectively. The voltage used here is the corrected voltage. Uncertainties in the current are <1 nA. b) The light intensity from 11 devices at 3 K on a G-center die all with a 3 μm implant window width and a 3 μm wire width shown as a function of ohmic separation. The error bars show one standard deviation of the photodiode's noise.

V. SUMMARY

The goal of this work was to fabricate CC-LED devices and study color centers by electroluminescence. The LED devices were varied with respect to their implant window width, wire width, and intrinsic region width. Electrical measurements of the CC-LEDs were taken by applying a voltage across the n-type and p-type regions of the devices to

collect and compare the I-V behavior for various design splits. This showed that both W-center and G-center LED devices exhibit the most linear and greatest above threshold slope for the devices with an overlap or no gap between the ohmics (p-n devices). The optical response of the devices was then studied by positioning a germanium photodiode over each die to measure the amount of light generated upon applying a voltage across the LED. This showed that the W-center devices with the overlapping ohmic regions provide the brightest light, while the G-center devices overlapping ohmic regions provide the dimmest light. A W-center CC-LED device was then measured in an optical cryostat and showed a ZPL at 1218 nm, the wavelength that is unique to W-center emission. The spectroscopic data on the G-center CC-LEDs is in progress. These efforts are a step towards the future of being able to couple light from silicon CCs to quantum dots all on-chip.

ACKNOWLEDGMENTS

We thank Dr. Jeffrey M. Shainline and Dr. Jeff Chiles at NIST for their technical discussions and insights. This is a contribution of the National Institute of Standards and Technology (NIST), an agency of the U.S. government.

AUTHOR DECLARATIONS

Conflicts of Interest

The authors have no conflicts to disclose.

DATA AVAILABILITY

The data that support the findings of this study are available from the corresponding author upon reasonable request.

REFERENCES

- ¹A. Durand, Y. Baron, W. Redjem, T. Herzig, A. Benali, S. Pezzagna, J. Meijer, A. Yu. Kuznetsov, J.-M. Gérard, I. Robert-Philip, M. Abbarchi, V. Jacques, G. Cassabois, and A. Dréau, *Phys. Rev. Lett.* **126**, 083602 (2021).
- ²S. M. Buckley, A.N. Tait, G. Moody, B. Primavera, S. Olson, J. Herman, K. L. Silverman, S. P. Rao, S. W. Nam, R. P. Mirin, and J. M. Shainline, *Opt. Express* **28**, 16057-16072 (2020).
- ³W. Redjem, Y. Zhiyenbayev, W. Qarony, V. Ivanov, C. Papapanos, W. Liu, K. Jhuria, Z. Y. Al Balushi, S. Dhuey, A. Schwartzberg, L. Z. Tan, T. Schenkel, and B. Kanté, *Nat. Commun.* **14**, 3321 (2023).
- ⁴G. Davies, *Phys. Rep.* **176**, 3 (1989).
- ⁵J.M. Shainline and J. Xu, *Laser Photonics Rev.* **1**, 4 (2007).
- ⁶C. Chartrand, L. Bergeron, K. J. Morse, H. Riemann, N. V. Abrosimov, P. Becker, H. -J. Pohl, S. Simmons, and M. L. W. Thewalt, *Phys. Rev. B.* **98**, 195201 (2018).
- ⁷L. W. Song, X. D. Zhan, B. W. Benson, and G. D. Watkins, *Phys. Rev. B.* **42**, 5765 (1990).
- ⁸A. Durand, Y. Baron, P. Idvarhelyi, F. Cache, K. V. R., T. Herzig, M. Khoury, S. Pezzagna, J. Meijer, J. -M. Hartmann, S. Reboh, M. Abbarchi, I. Robert-Philip, A. Gali, J. -M. Gérard, V. Jacques, G. Cassabois, and A. Dréau, arXiv, 2404.15069 (2024).
- ⁹D. D. Berhanuddin, M. A. Lourenço, R. M. Gwilliam, and K. P. Homewood, *Adv.*



This is the author's peer reviewed, accepted manuscript. However, the online version of record will be different from this version once it has been copyedited and typeset.
PLEASE CITE THIS ARTICLE AS DOI: 10.1116/6.0004055

Funct. Mater., **22**, 2709-2712 (2012).

¹⁰S. Buckley, J. Chiles, A. N. McCaughan, G. Moody, K. L. Silverman, M. J.

Stevens, R. P. Mirin, S. W. Nam, and J. M. Shainline, Appl. Phys. Lett. **111**, 14 (2017).

¹¹Y. Zhiyenbayev, W. Redjem, V. Ivanov, W. Qarony, C. Papapanos, J. Simoni, W. Liu,

K. Jhuria, L. Z. Tan, T. Schenkel, and B. Kanté, Opt. Express **31**, 8352-8362 (2023).